# Supplementary Figure 1

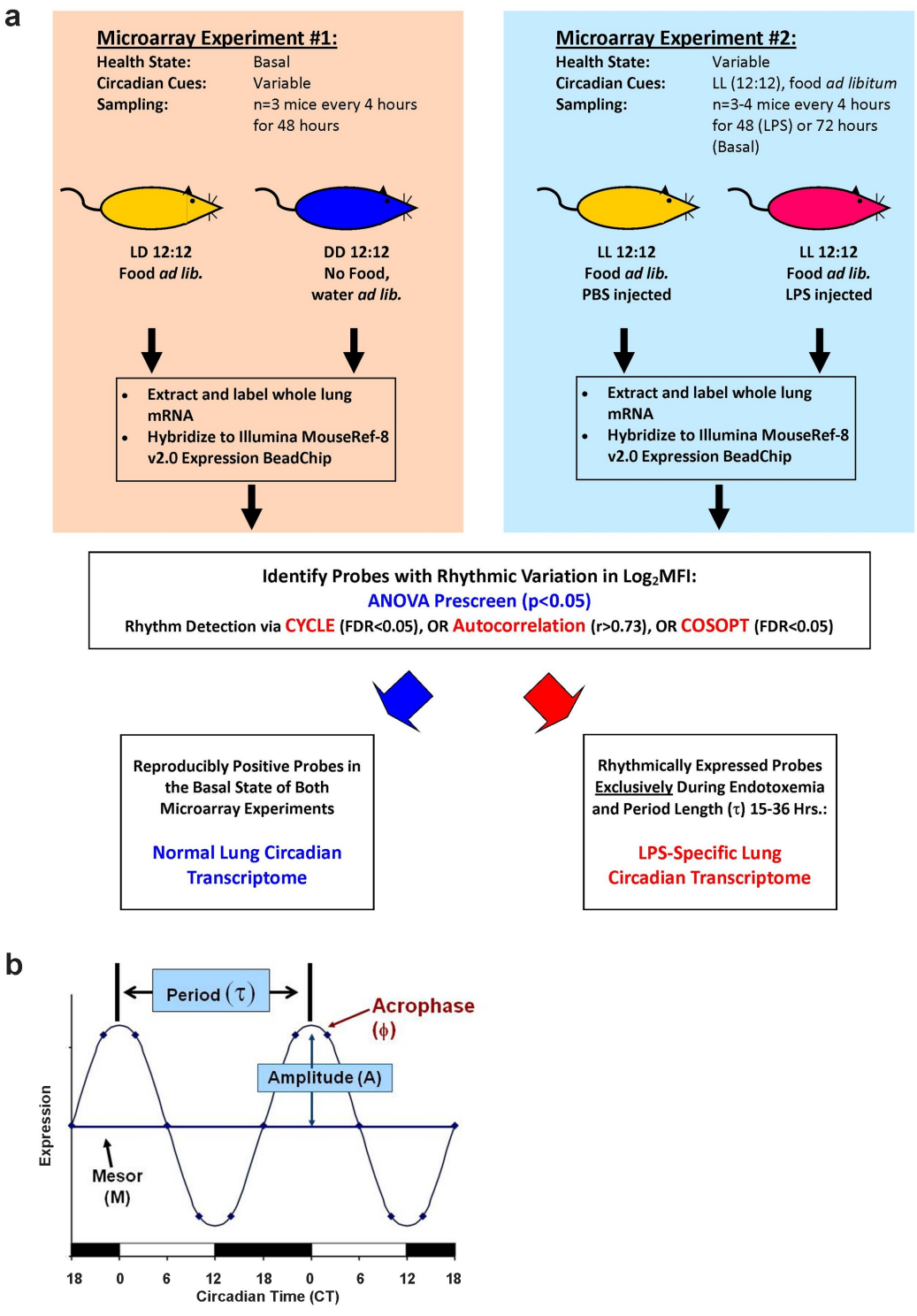


**Supplementary Figure 1** Experimental design for analyzing molecular circadian rhythms in mouse lung. (**a**) Schematic depiction of microarray time series analysis to identify the circadian transcriptome specific to the basal and endotoxemic states. Note that all tissues for metabolomic analysis and IHC were derived from the biological samples used for Microarray Experiment #2. (**b**) For each temporal pattern we then estimated 4 circadian parameters using COSOPT. These are: mesor (M, the average level around which the rhythm varies), amplitude (A, the maximum deviation from the mesor), period length (t, the duration of each cycle), and acrophase (f, the time at which expression is highest). We followed the standard convention of reporting times of day in units of Circadian Time (CT), where CT0 represents lights-on and CT12 lights-off.

# Supplementary Figure 2

**a. T=0 Post-LPS (CT10)**

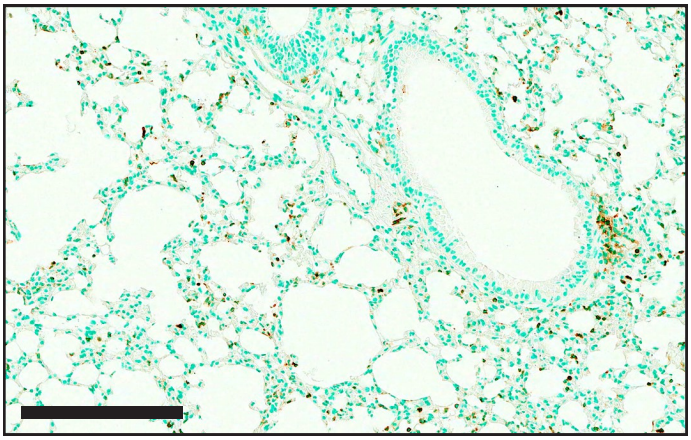

**b. T=28 Post-LPS (CT6)**

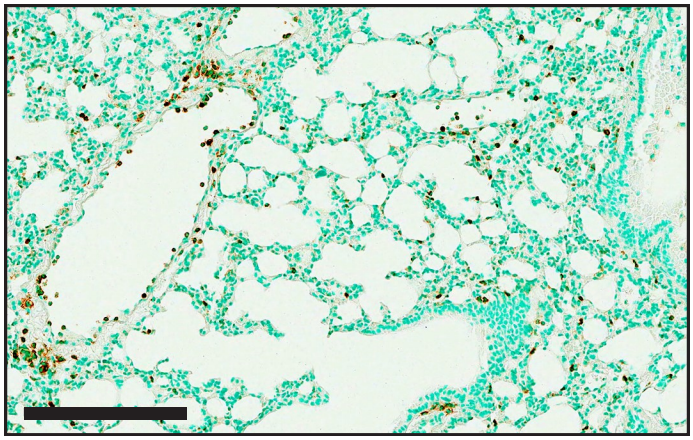

**c. T=44 Post-LPS (CT6)**

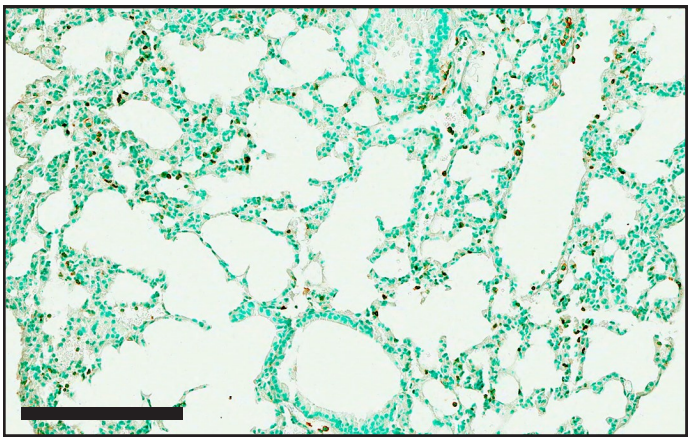

**d. Representative Survival Experiment**

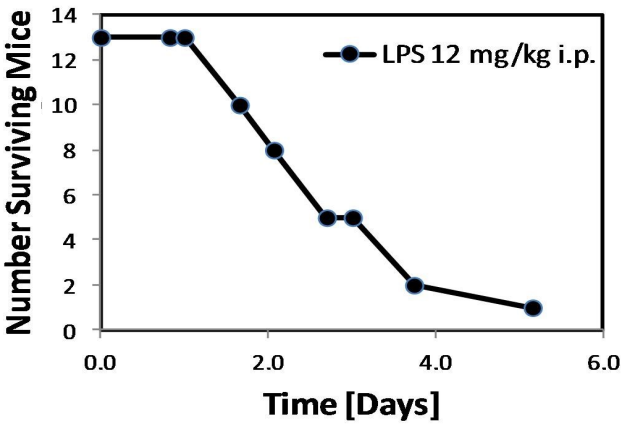


**Supplementary Figure 2** Characterization of endotoxemia dose used in this study. (**a-c**) Representative microscopic fields illustrating gross preservation of lung architecture in our model of endotoxemia throughout the period of observation. Brown pixels represent $CD45^{+}$ immunohistochemical stain. (**d**) Representative survival curve with the endotoxin lot and dosing used for genome-wide analyses.

# Supplementary Figure 3

## a Mesor (M) Distributions

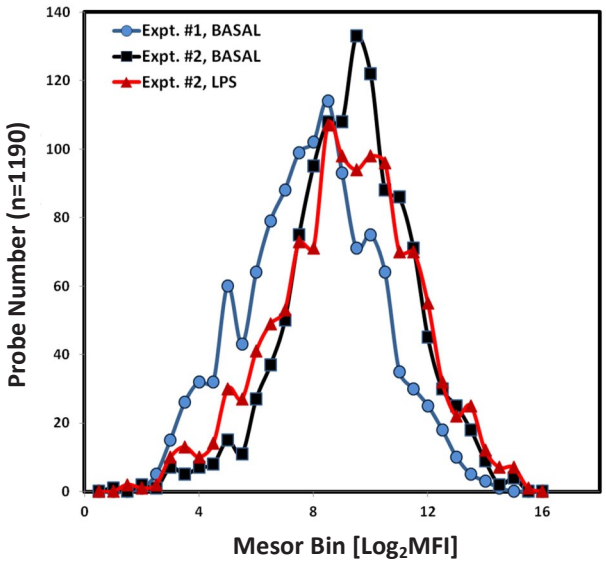


## b Mesor Δ Distributions

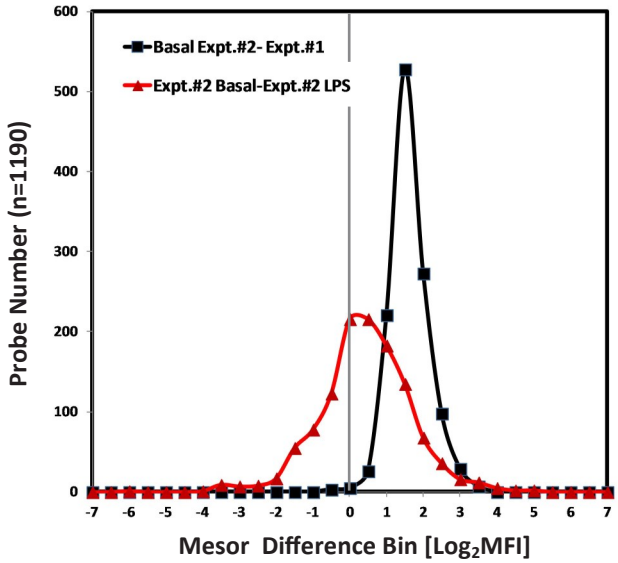


## c Amplitude (A) Distributions

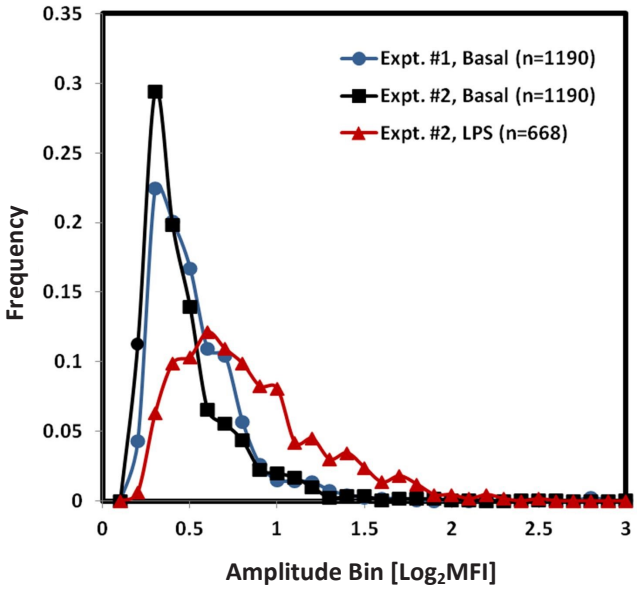


## d Amplitude Δ Distributions

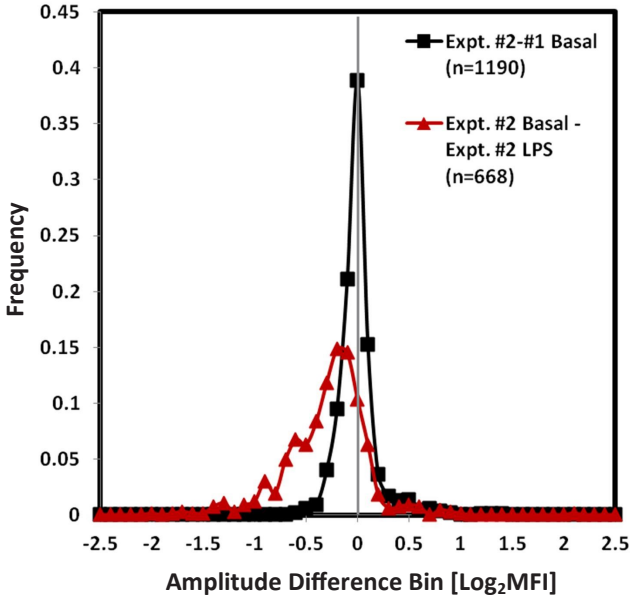


## e

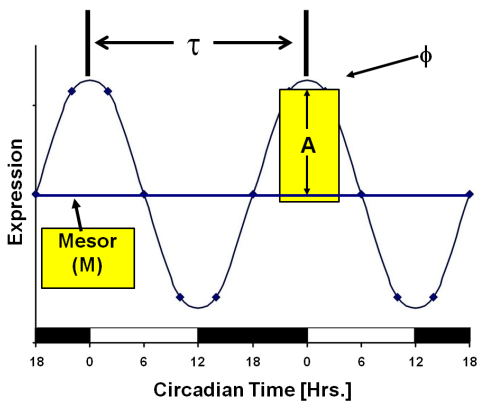

**Supplementary Figure 3** Endotoxemia does not strongly affect the time-averaged abundance (mesor) of circadian-regulated transcripts in mouse lung, or the magnitude of temporal variation (amplitude). (**a**) Histogram depicting the distribution of mesors for the 1190 microarray probes exhibiting circadian regulation in normal mouse lung. The light blue and black lines represent data from the basal groups of Microarray Experiments #1 and #2, respectively. The red line represents mesors from the endotoxemia group of Microarray Experiment #2. (**b**) Histogram depicting the distribution of mesor differences between health states. The black line represents mesor differences between basal groups of Microarray Experiments #1 and #2. The red line represents the mesor differences between basal and endotoxemia groups of Microarray Experiment #2. (**c**) Histogram depicting the distribution of amplitudes in the normal mouse lung circadian transcriptome (light blue and black lines), and during endotoxemia (red line). (**d**) Histogram depicting the distribution of amplitude differences between health states. The black line represents amplitude differences between basal groups of Microarray Experiments #1 and #2 (n=1190 probe pairs). The red line represents the difference in amplitudes between the basal and endotoxemia groups of Microarray Experiment #2 (n=668 probe pairs). (**e**) Schematic of an idealized waveform with the circadian rhythm characteristics of mesor and amplitude highlighted in yellow.

# Supplementary Figure 4

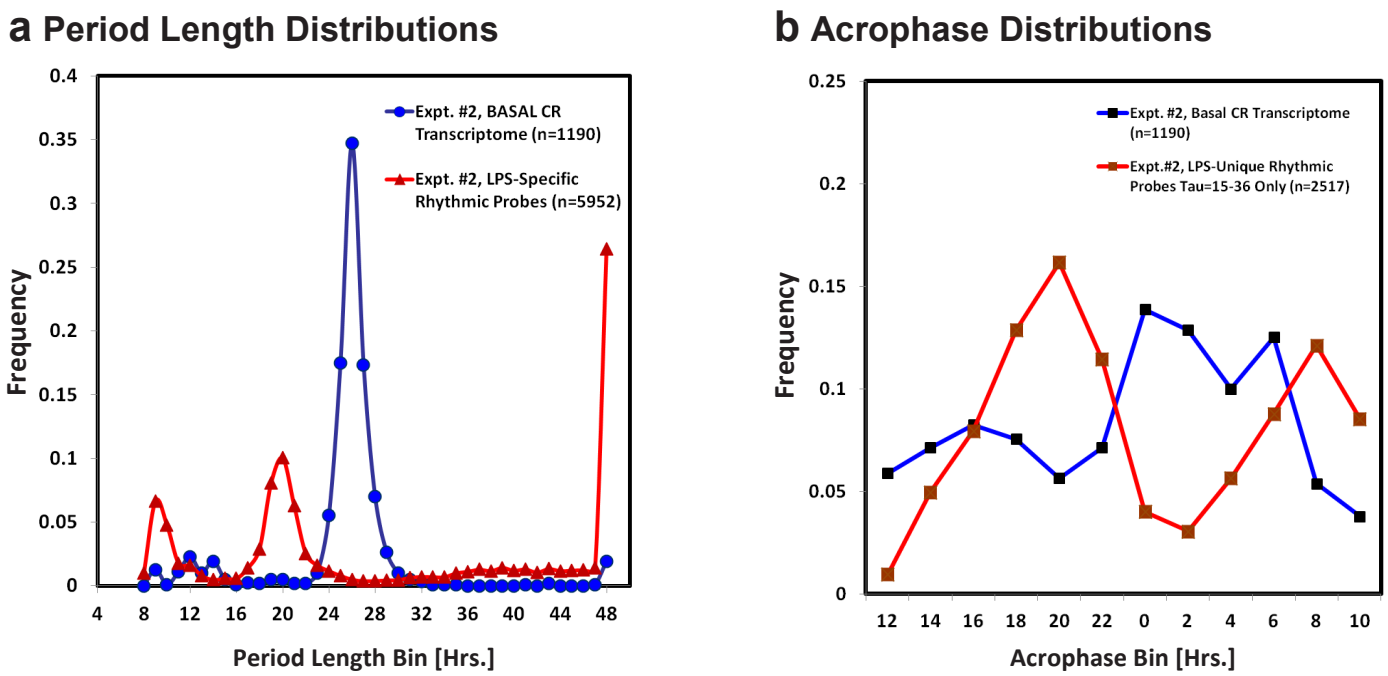


**Supplementary Figure 4** Rhythm parameter analysis of probes exhibiting periodic expression exclusively during endotoxemia. (**a**) Histogram comparison of period lengths associated with the basal lung circadian transcriptome (blue line) and probes that are exclusively periodic during endotoxemia (red line). Data from Microarray Experiment #2 is depicted. (**b**) Histogram comparison of acrophases associated with the basal lung circadian transcriptome (blue line) and probes that are exclusively periodic during endotoxemia (red line). For clarity, only probes associated with period lengths between 15-36 hours are depicted.

# Supplementary Figure 5

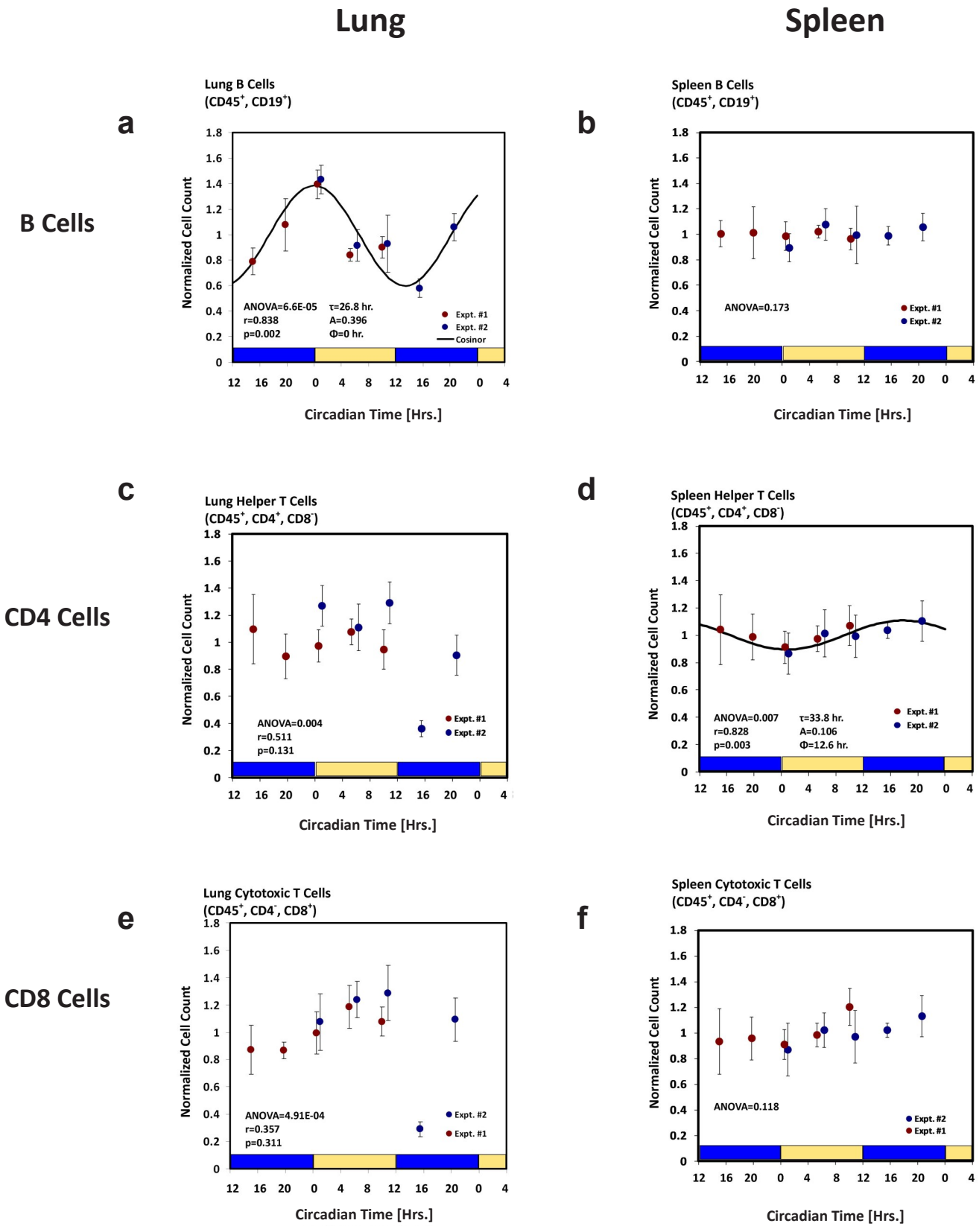

**Supplementary Figure 5** Circadian variation of lung lymphocyte subsets in healthy mice. Cell counts were determined via flow cytometry of dissociated whole lungs (**a, c, e**) and spleens (**b,d,f)** derived from the same animals and the time coordinates from 2 independent experiments were overlapped. Each point represents the mean of n=4-6 mice ± SE. For each experiment cell counts were normalized to the time-averaged mean to adjust for potential differences in instrument calibration between independent experiments. Cell populations depicted here include $CD45^{+}$-$CD19^{+}$ B-cells (**a**,**b**), $CD45^{+}$-$CD4^{+}$-$CD8^{-}$ T-cells (**c,d**), and $CD45^{+}$-$CD4^{-}$-$CD8^{+}$ T-cells (**e,f**). Significance values per one-way ANOVA, and rhythm parameters of the best-fit single-harmonic cosine curve are depicted within each figure panel where appropriate. See **Supplementary Fig. 10** for representative gates. Mice used for these experiments were housed under constant dark (DD 12:12) conditions.

# Supplementary Figure 6

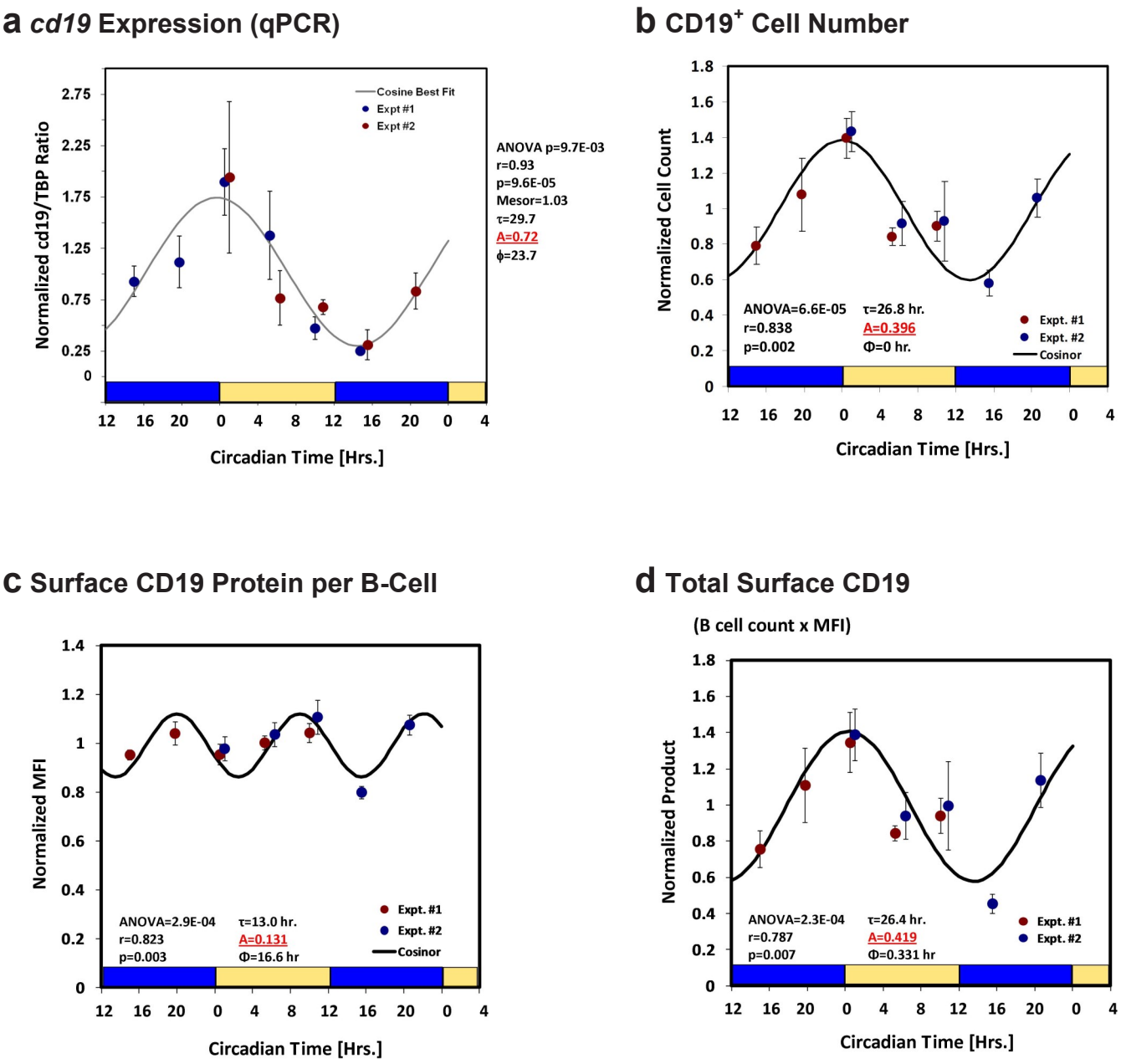


**Supplementary Figure 6** Oscillations in B-cell number drives the circadian expression pattern of cd19 in normal mouse lungs. (**a**) qPCR analysis of cd19 expression as a function of circadian time in basal mouse lung. Each data point represents mean cd19/tbp ratios ± SE from mouse lungs (n=4-6). Ratios were normalized to the time averaged mean for each of the independent experiments. (**b**) Lung B-cell number over time. This panel is the same as **Supplementary Fig. 5a** and is depicted here for ease of viewing. (**c**) CD19 Median fluorescence intensity (MFI) over time. Each point represents the mean of n=4-6 mice ± SE normalized to the time-averaged mean for each experiment. (**d**) The product of normalized B-cell count and normalized CD19 MFI. Significance values per one-way ANOVA, and rhythm parameters of the best-fit single-harmonic cosine curve are depicted. Mice used for these experiments were housed under constant dark (DD 12:12) conditions.

# Supplementary Figure 7

**a** Lung Alveolar Macrophages
(CD45$^+$, CD11c$^+$, Siglec F$^+$)

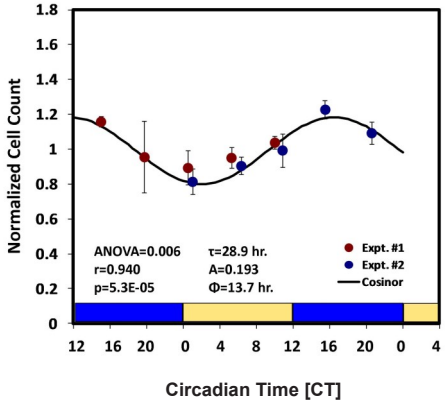


**b** Lung Monocytes
CD45$^+$, CD11b$^+$, Gr1$^-$

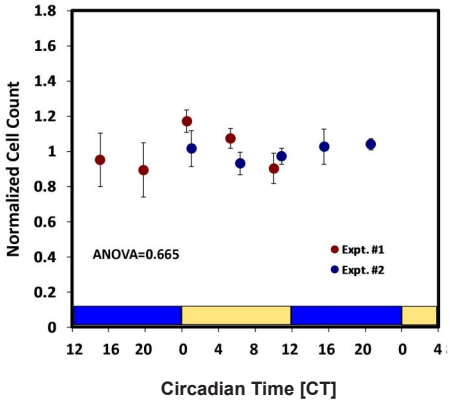


**c** Lung Gr1$^+$ Myelocytes
(CD45$^+$, CD11b$^+$, Gr1$^+$)

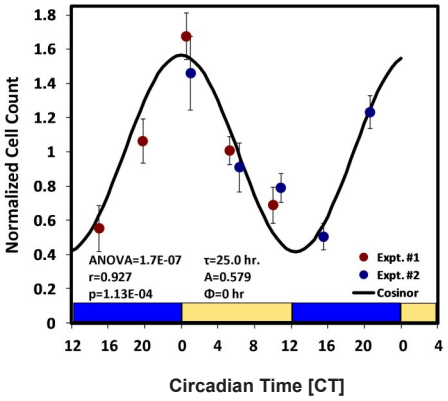


**d** Lung Epithelial Cells
(CD45$^-$, EPCAM$^+$)

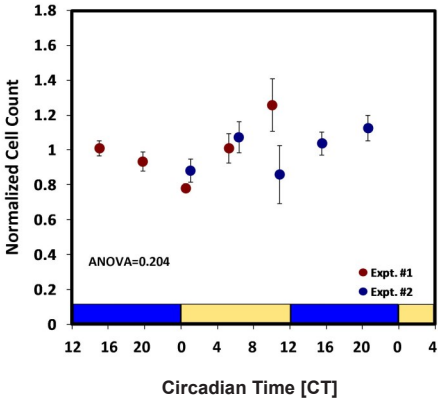


**e** Lung Endothelial Cells
(CD45$^-$, CD31$^+$)

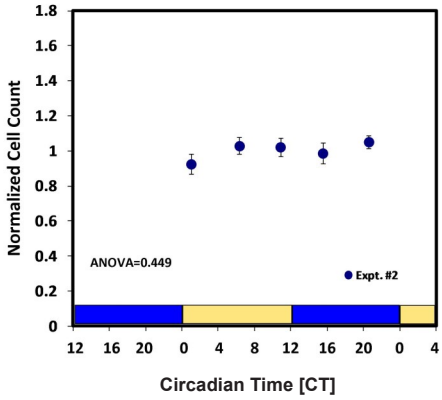

**Supplementary Figure 7** Circadian variation in lung myeloid, epithelial and endothelial cells. Cell counts were determined via flow cytometry of dissociated whole lung and the time coordinates from 2 independent experiments were overlapped as in **Fig. 5a**. Each point represents the mean of n=4-6 mice ± SE. For each experiment cell counts were normalized to the time-averaged mean to adjust for potential differences in instrument calibration between independent experiments. (**a**) Alveolar macrophages ($CD45^+$-Siglec $F^+$-$CD11c^+$); (**b**) Gr1- monocytes ($CD45^+$-$CD11b^+$-$Gr1^-$); (c) $Gr1^+$ granulocytes ($CD45^+$-$CD11b^+$- $Gr1^+$); (**d**) epithelial cells ($CD45^-$-$EpCAM^+$); (**e**) endothelial cells ($CD45^-$-$CD31^+$). See **Supplementary Fig. 10** for representative gates. Mice used for these experiments were housed under constant dark (DD 12:12) conditions.

# Supplementary Figure 8

**a Bmal1 (Basal), CT 6**

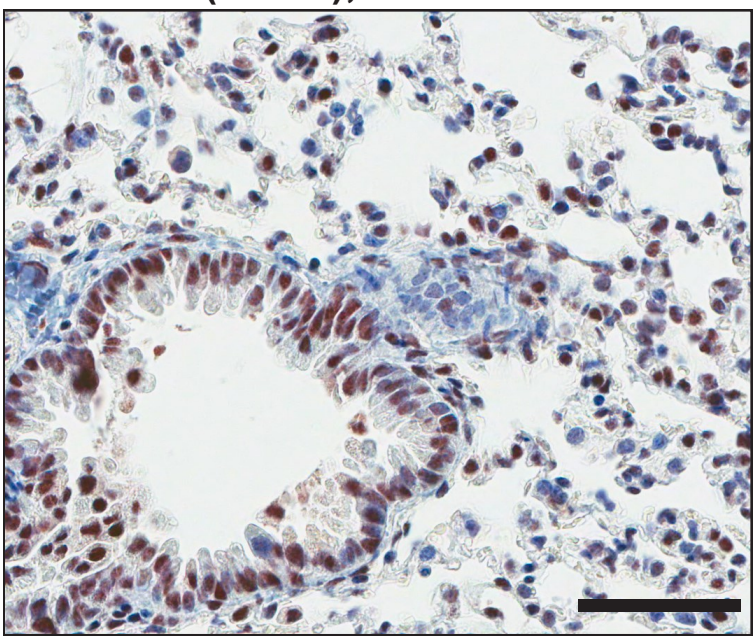

**b Bmal1 (LPS), CT 6**

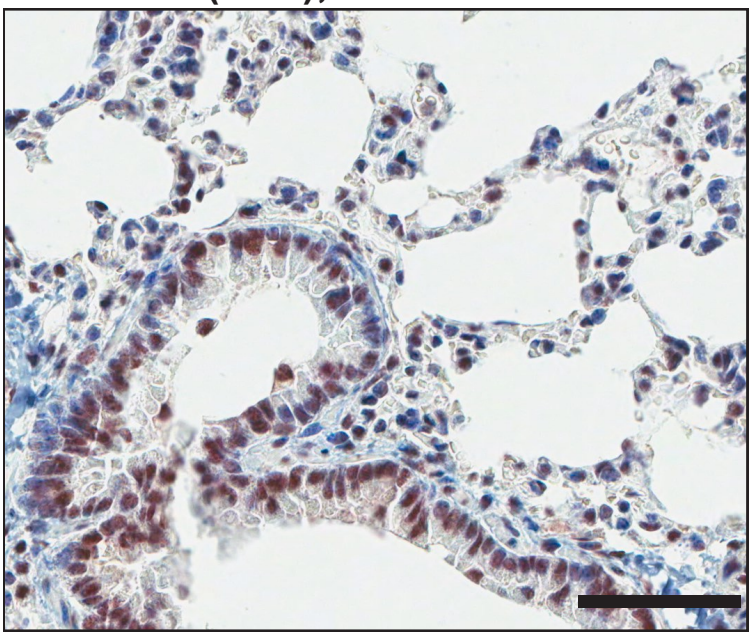

**Supplementary Figure 8** Representative slides depicting Bmal1 immunohistochemistry in lung samples used for Microarray Experiment #2. Red nuclear stain represents Bmal1 cross-reactivity. (**a**) Lung tissue from healthy mice at CT6. (**b**) Lung tissue from endotoxemic mice at CT6 (44 hours post-injection). Scale bar=60 μm.

# Supplementary Figure 9

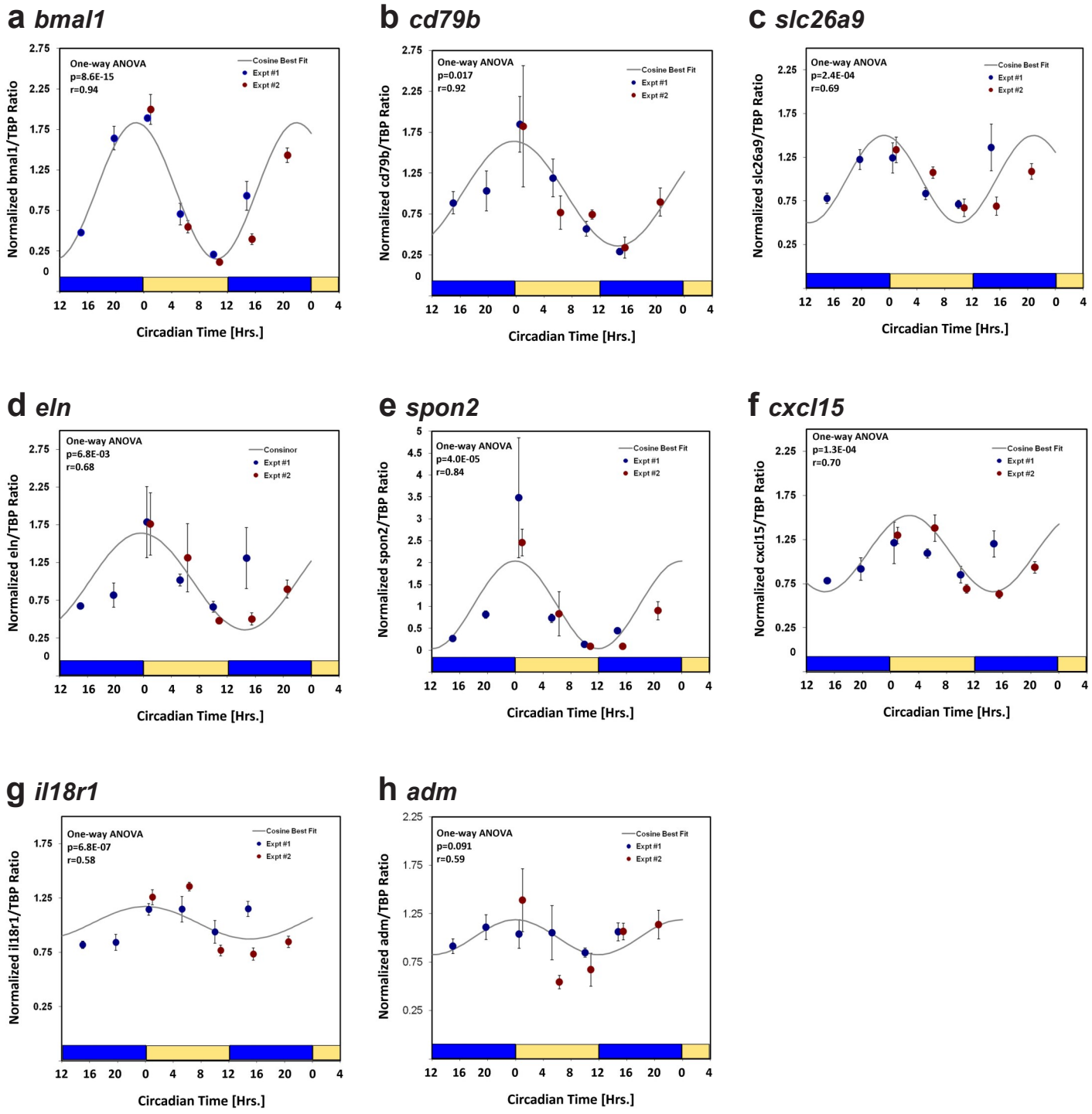


**Supplementary Figure 9** Quantitative PCR validation of the basal circadian transcriptome in mouse lung. Biological samples were obtained from two independent experiments (Experiments #1 and #2) used for flow cytometry analysis (**Fig. 5; Supplementary Figs. 5-7**). For each gene the data points represent the mean Ct ratio of n=4-6 right lower lobe fragments ± SE (using tbp as the housekeeping gene). To facilitate comparisons between experiments all ratios were normalized to the overall mean Ct ratio for each independent experiment and the time coordinates were overlaid. A best fit single-harmonic cosine curve is plotted in grey. Significance values (via one-way ANOVA) and goodness of fit to the cosine curve (Pearson's r) are depicted above each curve. (**a**) *bmal1*; (**b**) *cd79b*; (**c**) *slc26a9*; (**d**) *eln*; (**e**) *spon2*; (**f**) *cxcl15*; (**g**) *il18r1*; (**h**) *adm*. Note that mice used for these experiments were housed under constant dark (DD 12:12) conditions.

# Supplementary Figure 10

## a B-Cells
**($CD45^+$-$CD19^+$)**

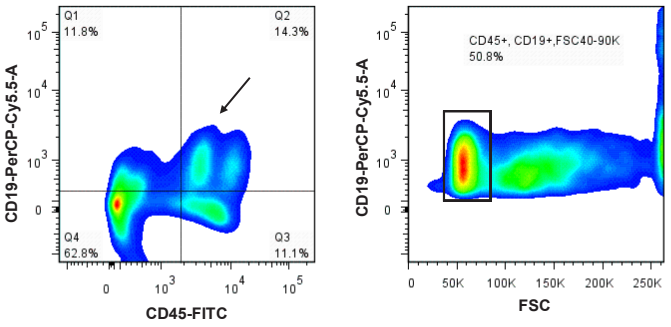


## b T-Cells
**($CD45^+$-$CD4^+$-$CD8^-$; $CD45^+$-$CD4^+$-$CD8^+$)**

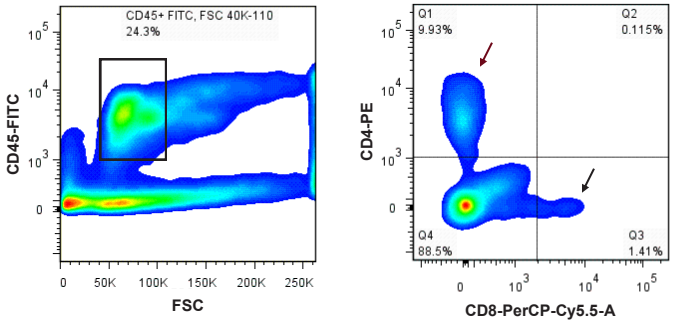


## c Alveolar Macrophages
**($CD45^+$-$CD11c^+$-Siglec-$F^+$)**

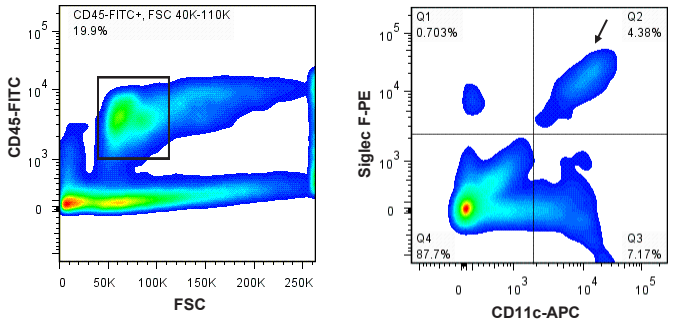


## d Monocytes and $Gr1^+$ Myelocytes
**($CD45^+$-$CD11b^+$-$Gr\text{-}1^-$; $CD45^+$-$CD11b^+$-$Gr\text{-}1^+$)**

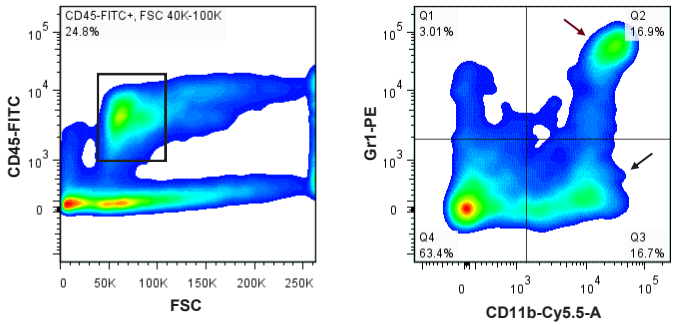


## e Epithelial Cells
**($CD45^-$-$EPCAM^+$)**

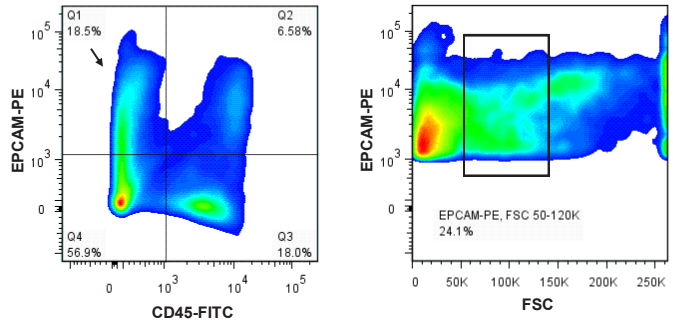


## f Endothelial Cells
**($CD45^-$-$CD31^+$)**

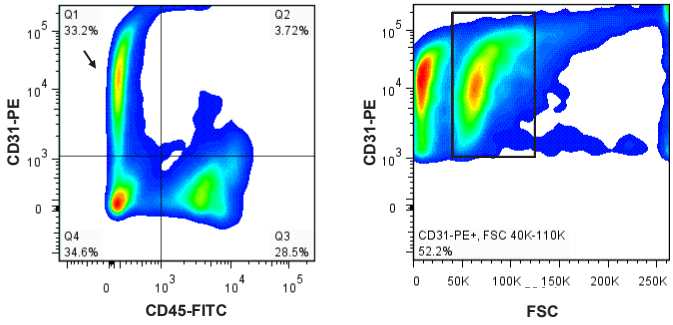


**Supplementary Figure 10** Representative gates used for flow cytometry. Arrows are depicted to indicate the quadrants of interest. Each panel represents the results from 50,000 events.

# Supplementary Figure 11

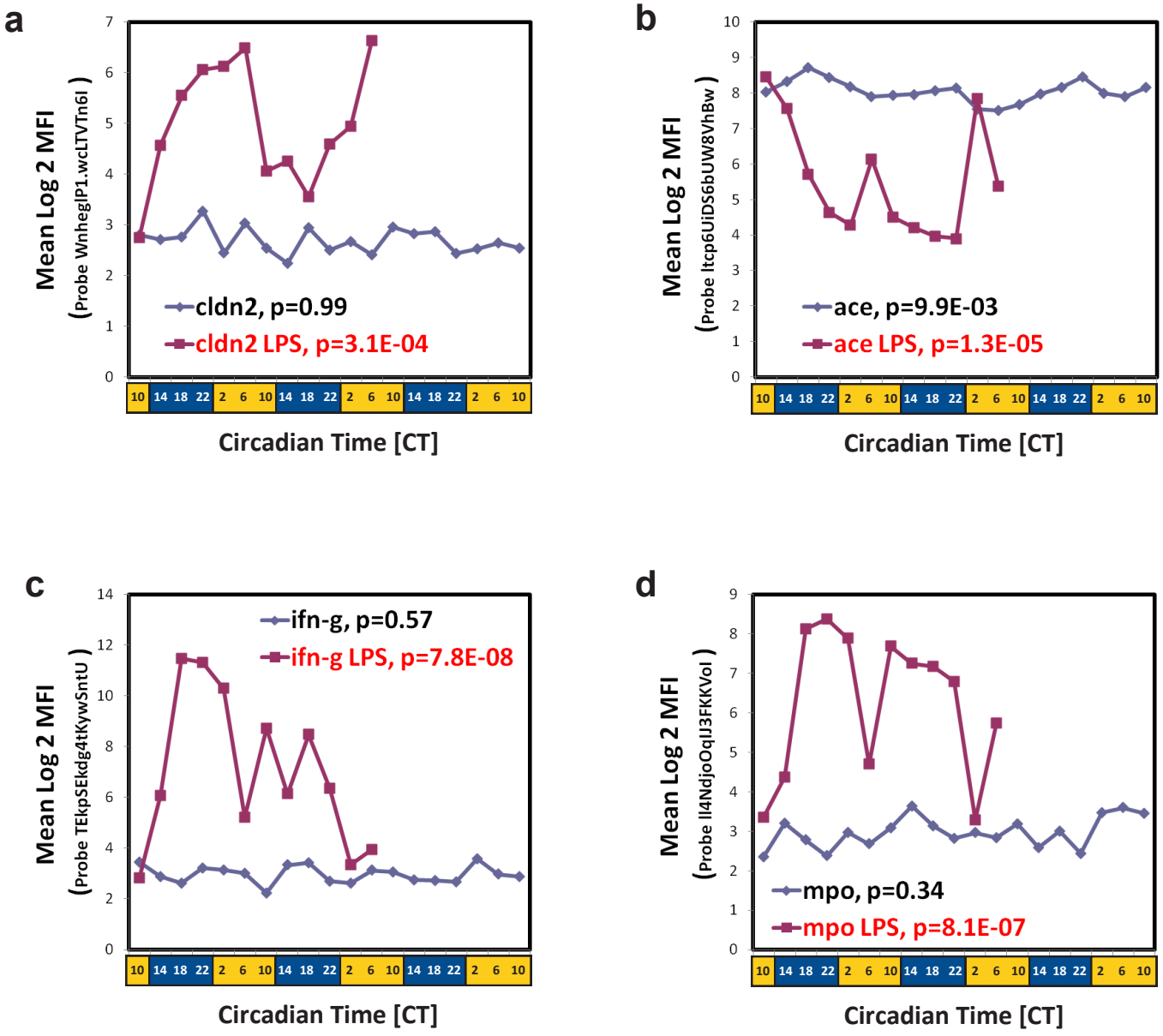


**Supplementary Figure 11** Expression of cldn2 (**a**), ace (**b**), *ifn-γ* (**c**), and *mpo* (**d**) in normal mouse lungs (blue line) and endotoxemic lungs (red line). Each data point represents the mean $Log_2$MFI (n=3-4 mice) derived from Microarray Experiment #2. Statistical significance as determined via one-way ANOVA is depicted.

# Supplementary Figure 12

## a Phospho-RS6

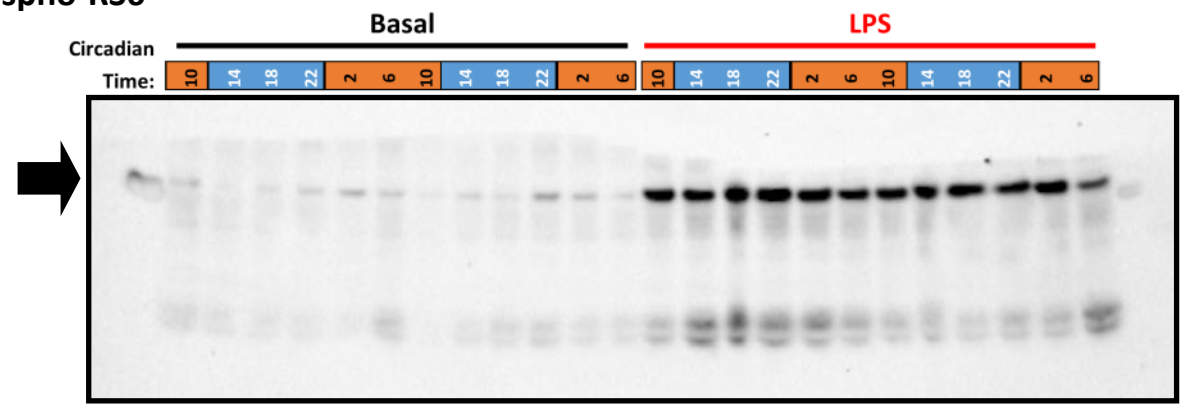


## b Total-RS6

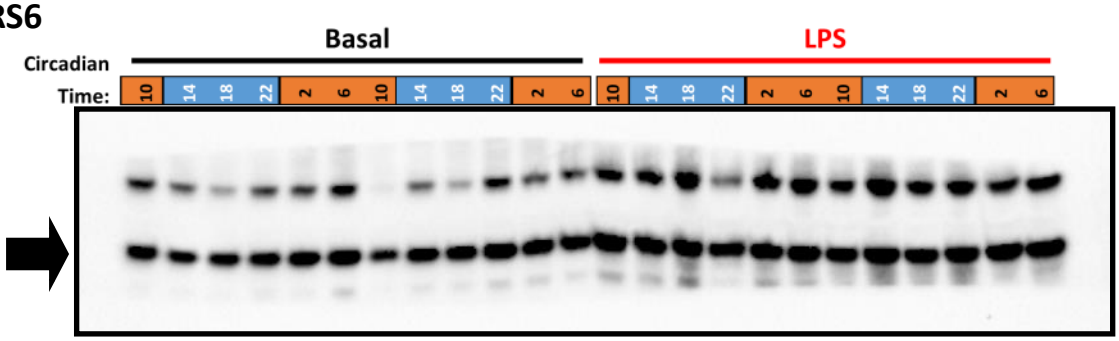


## c Phospho-AMPK

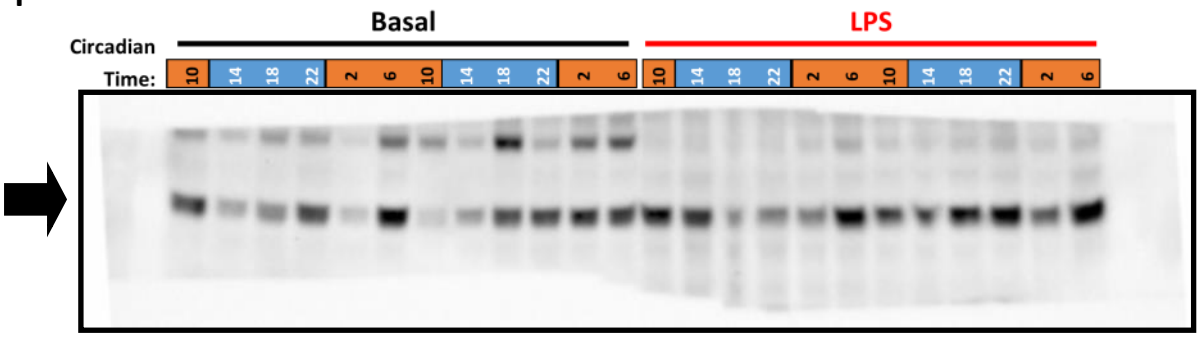


## d Total-AMPK

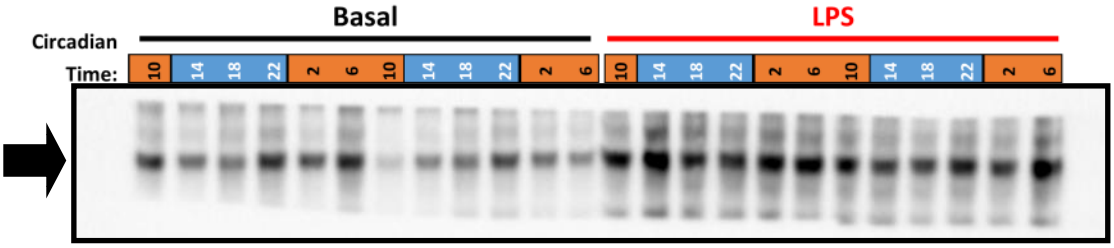


## e β-actin

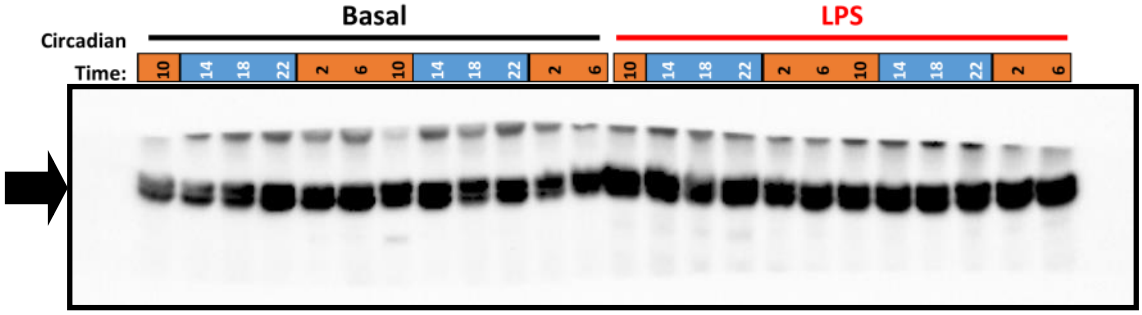

**Supplementary Figure 12** Full images for western blots presented in **Fig.** 8. Note that the PVDF membranes were cut to size prior to application of primary antibodies. (**a**) phospho-RS6, (**b**) total-RS6, (**c**) phospho-AMPK, (**d**) total-AMPK, (**e**) β-actin. The relevant band for each blot is denoted by an arrow.

**Supplementary Table 1**

| Organ Type | Species | Number of Genes Overlapping With Basal Mouse Lung Circadian Transcriptome [%] (n=1067) | Number of Genes Overlapping With Endotoxin-Specific Mouse Lung Circadian Transciptome [%] (n=2241) | References |
|---|---|---|---|---|
| **Mouse Lung Only** | - | 321 [30.0] | 963 [44.0] | |
| **Suprachiasmatic Nucleus** | Mouse | 93 [8.7] | 135 [6.0] | 1,2 |
| **Liver** | Mouse | 117 [11] | 100 [4.5] | 1-6 |
| **Kidney** | Mouse | 63 [5.9] | 73 [3.3] | 1 |
| **Aorta** | Mouse | 141 [13.2] | 141 [6.3] | 1 |
| **Skeletal Muscle** | Mouse | 56 [5.2] | 26 [1.2] | 1,5 |
| **Heart** | Mouse | 95 [8.9] | 108 [4.8] | 1,4 |
| **Adrenal Gland** | Mouse | 353 [33.1] | 373 [16.6] | 1,7 |
| **Brown Fat** | Mouse | 118 [11.1] | 114 [5.1] | 1,6 |
| **White Fat** | Mouse | 100 [9.4] | 72 [3.2] | 1,6 |
| **Calvarial Bone** | Mouse | 214 [20.1] | 184 [8.2] | 1,6 |
| **Preforntal Cortex** | Mouse | 83 [7.8] | 95 [4.2] | 1,8 |
| **Whole Brain** | Mouse | 135 [12.7] | 73 [3.3] | 1,9 |
| **Atrium** | Mouse | 101 [9.5] | 40 [1.8] | 1,10 |
| **Ventricle** | Mouse | 53 [5] | 16 [7.1] | 1,10 |
| **Liver (High Resolution)** | Mouse | 227 [21.3] | 238 [10.6] | 11 |
| **Colon** | Mouse | 72 [6.7] | 73 [3.2] | 12 |
| **Lung** | Rat | 113 [20.6] | 49 [2.2] | 13 |

Comparison of Mouse Lung Circadian Transcriptome in the Basal and Endotoxemic states to Other Circadian Datasets.

**Supplementary Table 2**

| Gene Symbol | Catalogue Number |
|---|---|
| *ace* | Mm00802048_m1 |
| *adm* | Mm00437438_g1 |
| *β-actin* | Mm00607939_s1 |
| *bmal1* | Mm00455950_m1 |
| *cd79b* | Mm00434143_m1 |
| *cldn2* | Mm00516703_s1 |
| *clock* | Mm00500226_m1 |
| *cxcl15* | Mm04208136_m1 |
| *eln* | Mm00514670_m1 |
| *gapdh* | Mm99999915_g1 |
| *ifnγ* | Mm01168134_m1 |
| *il18r1* | Mm00515178_m1 |
| *mpo* | Mm01298424_m1 |
| *slc26a9* | Mm00628490_m1 |
| *spon2* | Mm00513596_m1 |
| *tbp* | Mm00446973_m1 |

Taqman Primers used for qPCR Analysis in This Study

**Supplementary Table 3**

| Antibody | Vendor | Catalogue Number |
|---|---|---|
| CD4-PE | EBioscience | 12-0041-81 |
| CD8-PerCP-Cy5.5 | EBioscience | 12-0081-80 |
| CD45-FITC | EBioscience | 11-00451-81 |
| CD19-PerCP-Cy5.5 | EBioscience | 12-0041-81 |
| CD31-PE | EBioscience | 12-0311-81 |
| EPCAM-PE | EBioscience | 12-5791-81 |
| Siglec-F-PE | BD-Pharmigen | 552126 |
| CD11c-Alexa647 | EBioscience | 51-0114-80 |
| Gr1-PE | EBioscience | 25-5931-81 |

Fluorophore-Conjugated Antibodies Used for Flow Cytometry

**Supplementary Table 4**

| Target Cell for IHC | Antigen Retrieval | Primary Antibody | Secondary Antibody | Stain |
|---|---|---|---|---|
| B-Cells | Citrate pH 8 | αB220 (BD Pharmingen 550286) 1:200 for 60 minutes. | Rabbit α-rat 1:750 for 30 minutes; Leica Rabbit Refine for 30 minutes. | DAB for 5 minutes, hemotoxylin counterstain. |
| Granulocytes | EDTA pH 8.0 | αMPO (Dako A0398) 1:3500 for 60 minutes. | Leica Rabbit Refine for 30 minutes. | DAB for 5 minutes, hemotoxylin counterstain. |
| Endothelial Cells | Trypsin | αCD31 (Biocare CM303B) 1:50 for 120 minutes (reapplied after 60 minutes). | Rabbit α-rat 1:750 for 30 minutes; Leica Rabbit Refine for 30 minutes. | DAB for 5 minutes, hemotoxylin counterstain. |
| Hematopoietic Cells | None | αCD45 (BD Pharmingen 550539) 1:1000 for 60 minutes. | Rabbit α-rat 1:200 for 60 minutes; Vectastain Elite for 60 minutes. | DAB for 5 minutes, methyl green counterstain. |
| $Bmal1^{+}$ Cells | EDTA pH 8.0 | αBmal1 (Santa Cruz sc-48790) 1:100 for 60 minutes. | Leica Rabbit Refine for 30 minutes. | DAB for 5 minutes, hemotoxylin counterstain. |

Antibodies Used for Immunohistochemistry

## SUPPLEMENTARY REFERENCES


1. Yan, J., Wang, H., Liu, Y. & Shao, C. Analysis of gene regulatory networks in the mammalian circadian rhythm. *PLoS Comput Biol* **4**, e1000193 (2008).
2. Ueda, H.R.*, et al.* A transcription factor response element for gene expression during circadian night. *Nature* **418**, 534-539 (2002).
3. Panda, S.*, et al.* Coordinated transcription of key pathways in the mouse by the circadian clock. *Cell* **109**, 307-320 (2002).
4. Storch, K.F.*, et al.* Extensive and divergent circadian gene expression in liver and heart. *Nature* **417**, 78-83 (2002).
5. Miller, B.H.*, et al.* Circadian and CLOCK-controlled regulation of the mouse transcriptome and cell proliferation. *Proc Natl Acad Sci U S A* **104**, 3342-3347 (2007).
6. Zvonic, S.*, et al.* Characterization of peripheral circadian clocks in adipose tissues. *Diabetes* **55**, 962-970 (2006).
7. Oster, H., Damerow, S., Hut, R.A. & Eichele, G. Transcriptional profiling in the adrenal gland reveals circadian regulation of hormone biosynthesis genes and nucleosome assembly genes. *J Biol Rhythms* **21**, 350-361 (2006).
8. Yang, S., Wang, K., Valladares, O., Hannenhalli, S. & Bucan, M. Genome-wide expression profiling and bioinformatics analysis of diurnally regulated genes in the mouse prefrontal cortex. *Genome Biol* **8**, R247 (2007).
9. Maret, S.*, et al.* Homer1a is a core brain molecular correlate of sleep loss. *Proc Natl Acad Sci U S A* **104**, 20090-20095 (2007).
10. Bray, M.S.*, et al.* Disruption of the circadian clock within the cardiomyocyte influences myocardial contractile function, metabolism, and gene expression. *Am J Physiol Heart Circ Physiol* **294**, H1036-1047 (2008).
11. Hughes, M.E.*, et al.* Harmonics of circadian gene transcription in mammals. *PLoS Genet* **5**, e1000442 (2009).
12. Hoogerwerf, W.A.*, et al.* Transcriptional profiling of mRNA expression in the mouse distal colon. *Gastroenterology* **135**, 2019-2029 (2008).
13. Sukumaran, S., Jusko, W.J., Dubois, D.C. & Almon, R.R. Light-dark oscillations in the lung transcriptome: implications for lung homeostasis, repair, metabolism, disease, and drug action. *J Appl Physiol* **110**, 1732-1747 (2011).